

# A LIGHT-WEIGHT HYPERSONIC INFLATABLE DRAG DEVICE FOR A NEPTUNE ORBITER

Angus D. McRonald

## ABSTRACT

The author has analyzed the use of a light-weight inflatable hypersonic drag device, called a ballute, for flight in planetary atmospheres, for entry, aerocapture and aerobraking. Studies to date include Mars, Venus, Earth, Saturn, Titan, Neptune and Pluto, and data on a Neptune orbiter will be presented to illustrate the concept at a large entry speed. For a Neptune orbiter a conventional rigid lifting entry body requires about 40% of the entry mass to be in the thermal shield and structure to take the pressure and thermal loads, and analysis indicates that the ballute mass for the same task may be about half this value. The main advantage of using a ballute is that aero deceleration and heating in atmospheric entry occur at much smaller atmospheric density with a ballute than without it. For example, if a ballute has a diameter 10 times as large as the spacecraft, for unchanged total mass, entry speed and entry angle, the atmospheric density at peak convective heating is reduced by a factor of 100, reducing the peak heating by a factor of 10 for the spacecraft, and a factor of about 30 for the ballute. Consequently the entry payload (descent probe, orbiter, etc) is subject to much less heating, requires a much reduced thermal protection system (possibly only an MLI blanket), and the spacecraft design is therefore relatively unchanged from its vacuum counterpart. By making the ballute large enough one can make the heat flux on the ballute small enough to be radiated at temperatures below 800 K or so. Also, the heating may be reduced further because the ballute enters at a more shallow angle than a solid vehicle, even allowing for the increased delivery angle error that one expects at shallow entry, for a given error in the target plane. Added advantages are less mass ratio of entry system to total entry mass, and freedom from the low-density instability problem that conventional rigid bodies suffer, since the vehicle attitude is determined by the ballute, which is usually released at continuum conditions. The ballute derives an entry corridor for aerocapture by entering on a path that would lead to entry, and releasing the ballute adaptively, responding to measured deceleration, to achieve the desired orbiter exit conditions. The author will discuss presently available ballute materials and a development program of aerodynamic tests and materials that would be required for ballutes to achieve their full potential.

## PRIOR BALLUTE STUDIES

Ballutes seem to have been invented in the forties and fifties to reduce the ground impact speed of empty sounding rockets or rocket casings. The investigators probably discovered that the mass of a ballute, inflated at high altitude, to slow a returning high altitude sounding rocket was less than the mass of a necessarily stronger parachute system that would open at low Mach number and high pressure. In the late sixties studies and wind tunnel tests were performed (1,2) by

---

Angus D. McRonald is a Senior Member of the Technical Staff at the Jet Propulsion Laboratory of the California Institute of Technology. The research described in this paper was carried out at the Jet Propulsion Laboratory, California Institute of Technology, under contract of the National Aeronautics and Space Administration.

Goodyear and NASA Langley with a view to using ballutes to assist deceleration of the Viking landers at Mars, but these ballutes were deployed after peak deceleration and heating, thus having limited potential to change the entry trajectory. A mushroom shape was found to be more stable than a sphere. In 1976 the authors of Ref. 3 proposed to use a ballute inflated prior to entry into Venus. They proposed a ballute of mass of over 300 kg and computed the ablation during entry, and evaluated some candidate materials. In the mid eighties studies of ballute materials were performed at NASA Langley, but again the concept was to deploy ballutes after peak entry deceleration and heating. In recent years NASA Ames has studied drag modulation of vehicles equipped with inflatable components (Ref. 4).

## RECENT STUDIES

In the past five years the author has studied the use of ballutes for aerocapture and entry at several planets, including a Mars orbiter and a Pluto lander, both reported in Ref. 5, and several ballutes for a Venus sample return mission, reported in Ref. 6. In recent years two materials that can be produced as thin films capable of temperatures on the order of 500 C are available (Ref. 7) - Kapton, which has strength 5600 psi (Ref. 7) and PBO (Polybenzoxazole, a liquid crystal polymer), available as fibers with a useful strength at 600 C, to function as a net to hold the ballute.

## BALLUTE SHAPES

The ballute concept is illustrated in Fig. 1. Although a ballute greatly reduces the peak convective heating (and also the radiative heating), there is only a small reduction in the peak g load due to drag, and therefore the ballute must be enclosed in a net that surrounds the ballute and communicates the total drag force to the payload. A ballute deployed from the rear of a payload, as illustrated in Fig. 1(a) has the advantage that the heating rate on the payload is reduced to the ballute level, but release of the ballute in aerocapture may not be easy. In Fig. 1(b) the ballute is let out on a tether, so that release is easy. Figure 1(c) shows a lens (or pancake) shape, which is more efficient than a sphere as a drag device, having a higher drag coefficient  $C_d$  (about 2 instead of 0.9) and a smaller (fabric) surface area (about half that of a sphere). Figure 1(c) can also be a disk with an outer ring, is similar to a lens in regard to drag area, but has even less material. For the lens and the disk one needs inflatable tubing deployed from the rear of the payload to help deploy the lens and disk ballute material in vacuum prior to entry. There is evidence (Ref. 8) that in conditions where a strong bow shock is formed ahead of the payload, there will be interaction with the bow shock of the ballute, leading to flow instability in the form of oscillations between different modes, perhaps sufficiently serious to invalidate accurate measurement of ballute drag. The remedy suggested is to have a ring ballute as in Fig. 1(d). Also, to avoid heating peaks at the edges (Ref. 9), the circular disk of Fig. 1(c) and the annular disk of Fig. 1(d) require inner and outer rings of diameter about 10% of the disk dimension. In the analysis below it is assumed that the inner hole is of radius one half of the outer radius, and for this disk with rings of appropriate size the total surface area of ballute material is 1.47 of the simple frontal area.

## AEROCAPTURE

To find the ballute size and mass for Neptune, it is appropriate to begin by evaluating the velocity loss in a pass through the atmosphere, with  $B = m/CdA$ , where  $m$  is the entry mass,  $Cd$  is the hypersonic drag coefficient, and  $A$  is the frontal area of the ballute, and the entry angle as parameters. Figure 2 shows the delta-V loss in an atmospheric pass, as a function of the entry angle, for a number of ballutes with various values of  $B$ . Figure 2 (a) relates to Neptune with inertial entry speed 28.3 km/s at altitude 1000 km, and for Fig. 2 (b) the entry speed is 32.0 km/s. The Neptune atmosphere model has molecular weight 2.38, composed of H<sub>2</sub> and He (0.69/0.31) by mass and (0.87/0.13) by volume (Ref. 10). The equivalent  $V_{inf}$  = speed at infinity of the two entry speeds are 16.1 and 22.0 km/s, respectively, representing a probable range for future fast travel to Neptune. Neptune has a speed of rotation on the equator of about 2.3 km/s, and the trajectories assumed a downwind entry with rotation speed of 2.265 km/s, a value somewhat less than 2.3 km/s. The graphs of delta-V loss take the form of steep, almost straight lines, and one can see that for a ballute retained for the whole pass the error in exit speed would be very great for a small error in entry angle. The remedy to this problem is to measure the velocity loss during the pass, and release the ballute when the chosen exit conditions are predicted, without the ballute from that time on. To aerocapture into a chosen orbit a certain delta-V is to be lost. For example, the inertial exit speed at altitude 1000 km for Neptune is 23.27 km/s just to capture into a long-period elliptic orbit, and is 16.45 km/s for a close circular orbit., and these are marked on Fig. 2 (a) and (b). To perform aerocapture with a ballute one would choose an entry angle to give at least the minimum delta-V that one wishes for a complete atmospheric pass, allowing for error in delivery (i.e., entry angle error) and for difference between the assumed atmosphere and the actual atmosphere. For a given known entry mass,  $m$ , one evaluates trajectories with increasing size (decreasing  $B = m/CdA$ ). From the trajectory one can find the peak heating rate for a particular size of ballute, and from a radiative balance one finds the peak temperature that the ballute would experience. Presently available ballute materials have a peak temperature limit of about 500 C.

## AEROCAPTURE TRAJECTORIES

Aerocapture trajectories were computed for the five ballute sizes of Fig. 3.. Figure 3a is for  $V_e = 28.3$  km/s, and shows the exit speed for release of the ballute at  $V = 20$  km/s, with a value of  $B = 120$  kg/m<sup>2</sup> for the orbiter alone. It can be seen that there is now an entry angle corridor, about 2 deg wide, with a small slope. It will be seen below that for a range of entry mass ballute number 4 is a likely choice, and there is a corridor of about  $\pm 1$  deg, equivalent to an error in the  $B$  plane (target plane) of more than 300 km, for entry angle 8.5 deg. Figure 3b shows similar plots of the exit speed for  $V_e = 32.0$  km/s and for two ballute release speeds, 20 and 22 km/s. Figure 4a shows the peak stagnation pressure, Figure 4b shows the peak stagnation point convective heating rate of a reference body with nose radius 0.43 m flying the same trajectory as the ballute, as a function of the entry angle, for the five ballutes and the two entry speeds. From this one

can compute the peak convective heating rate for the ballute, and hence the maximum temperature prior to ballute release. Figure 4c shows the peak g-load, and Fig. 4d shows the peak free-molecular heating rate for the same conditions as in Fig. 4e = 28.3 and 32.0 km/s. Figure 6a shows the peak temperature of the ballute disk for  $V_e = 28.3$  km/s, for emissivity = 0.7, radiating on both sides of the ballute, for the 5 ballute sizes, as a function of the ballute radius, for 3 values of entry mass,  $m = 100, 400$  and  $1600$  kg. Figures 6b, 6c and 6d show the maximum temperatures for  $V_e = 28.3$ , emissivity 0.5, for  $V_e = 32.0$  and emissivity 0.7, and for  $V_e = 32.0$  and emissivity 0.5.

## BALLUTE HEATING

Table 1. Relative Stagnation Point Convective Heating Rate for Several Gases (Ref. 11)

Gas	Air	Co2	H2/He Mass Ratio			
			0.15	0.35	0.65	0.899 (Neptune)
Relative Heating Rate	.1113	.1210	.0657	.0547	.0469	(.0400)

Reference 9 has given a heating distribution for a disk at peak heating conditions for Venus, and the reference heating used above is for air at Neptune conditions, with a H<sub>2</sub>/He mass ratio of 0.87/0.13. Table 1 shows relative convective heating for 3 He/He gases, CO<sub>2</sub> and air. From these one can estimate that the Neptune H<sub>2</sub>/He mixture will have a value of about 0.040 relative to Table 1. Using the well known dependence of convective heating on square root of (density/radius) and cube of velocity, and a peak heat flux for a disk in Venus aerocapture, one can determine that there is a factor of about 0.8 relating a sphere to a disk in regard to peak heating, and also that the heating rate for the Neptune atmosphere is  $0.040/0.1113 =$  i.e., about 0.36 of the reference (air) value used here. It is assumed that radiative heating on the ballute will be relatively small, since it is thought to be a few percent of convective heating at these speeds for Neptune for a body of dimension 1 m, and the use of a ballute has decreased the density for peak heating by perhaps 400 and increased the thickness of the shock layer by 20, so that the radiative source is now a volume source of relatively low intensity.

## BALLUTE COMPONENTS

The ballutes computed here are assumed to have five components: 1) the drag disk of radius R (Kapton, 10 gm/m<sup>2</sup> sheet), including the inner and outer ring material, which adds a factor 0.47 more to the disk area; 2) a net (PBO fibers) whose total cross sectional area must support the total peak drag force; a tensile strength of 56 kg/mm<sup>2</sup> is assumed, and the length is 6R, where R is the disk outer radius; 3) tubing (PBO) to be inflated prior to entry to help the ballute material deploy to the desired shape in vacuum (assumed to be ten disk diameters in length, pressurized to 1 atm in 5 cm diameter tubing of thickness 2 mil, a thickness that gives 10 times the burst pressure cold, and equal to it when at 600 C); (4) an amount of pressurant helium gas sufficient to inflate the tubing to 1 atm and the rings of the disk to about 100 N/m<sup>2</sup> (at least as great as the peak shock

layer pressure); and (5) a He bottle of mass equal to that of the He. The tensile strength assumed for the net is the room temperature value; behind the ballute the net is shielded from stagnation heating, and in front it is assumed that the net material is shielded by the tubing or in some other way. The materials of the ballute were assumed to be 10 gm/m<sup>2</sup> Kapton. The relative mass of the components varies with the ballute radius, R. The tubing and the net vary as R, the net varies also as g<sub>max</sub> and m, the ballute fabric mass varies as R squared, and the He mass varies as R in the tubing and as R squared in the lens or rings. It turns out that the He gas mass is relatively small, and only the three main components - ballute, net and tubing will be significant here. Five values of m/CdA were computed, and for each of these values one can vary m and thus R, so that the fraction of mass required for the ballute and its components varies with the assumed entry mass, m.

## BALLUTE MASS

Since the governing parameter for a ballute trajectory is  $B = m/CdA$ , it is useful to begin with a simple mass of 100 kg and a chosen  $B = 0.5 \text{ kg/m}^2$ , for example (ballute number 1). Then, with  $Cd = 2$  for a disk or lens, and  $A =$  the area of the circle, one can find the corresponding radius R. From the value of  $q_{refmax}$  one can compute the peak ballute heating and the equilibrium radiative peak temperature,  $T_{max}$ , and then find a ballute B value that brings  $T_{max}$  below 500 C (773 K). Thereafter one can increase A to suit the desired entry mass m. The basic ballute mass components (excluding He gas bottle, ballute release device, ballute cover or container) are shown in Table 2 for representative Venus direct entry at  $V_{e140} = 11.5 \text{ km/s}$  and  $m = 100 \text{ kg}$ .

Table 2. Ballute for Direct Neptune Aerocapture at  $V_e = 28.3 \text{ km/s}$ , based on 100 kg entry mass

B=m/CdA,kg/m <sup>2</sup>	0.5	0.25	0.10	0.05	0.025
Radius R, m	6.52	9.21	13.0	20.6	29.1
Entry angle, deg	9.75	9.5	9.0	8.75	8.25
p <sub>max</sub> , N/m <sup>2</sup>	125	68	29	10	5
q <sub>refmax</sub> ,W/cm <sup>2</sup>	137	99.2	60.2	38.1	25.2
g <sub>max</sub>	13.1	14.1	12.2	12.5	11.0
q <sub>f</sub> ,W/cm <sup>2</sup>	126	69	28	11.1	4.8
mass of disk,kg	1.47	2.94	5.8	9.30	9.42
mass of net, kg	1.03	1.45	2.05	3.24	4.58
mass of tubing, kg	1.37	2.09	2.55	4.15	5.16
total mass,kg	3.98	6.64	10.71	17.06	23.49
(excluding He bottle and fittings, and He for tubing and rings, which are relatively small)					
T <sub>max</sub> , degK (e=0.7)	1271	1123	950	787	691

These masses and the values of R are for an entry mass m of 100 kg nominal. They scale as: area with m, lens mass with m, net mass with m and R, tubing mass with R, He mass with m for rings and R for tubing.

### NEPTUNE BALLUTE MASSES

From the trajectory data for direct hyperbolic entry, given an entry mass, one can evaluate the ballute radius and hence the peak radiative equilibrium temperature. The peak temperature,  $T_{max}$ , is shown in Fig. 6 for entry masses of 100, 400 and 1600 kg, and also for  $V_e = 28.3$  and 32.0 km/s. Values of  $T_{max}$  are shown for two values of the ballute material emissivity, 0.5 and 0.7, believed to bracket the true value for films of the thickness considered here, 7 micron (10 gm/m<sup>2</sup>).

The ballute mass fraction of the entry mass, determined from the components shown in Table 2, is shown in Fig. 7 as a function of ballute radius for entry mass of 100, 400, and 1600 kg for direct entry. From Fig. 6, choosing a  $T_{max}$ , e.g., 500 C for Kapton, one can evaluate the ballute radius for the appropriate entry mass and speed, and from Fig. 7 one can evaluate the mass fraction = ballute system mass/entry mass for that temperature, mass and speed.

Typical (middle of the corridor) ballute radii and mass fractions are shown in Table 3 for the values of  $V_e$ , two values of emissivity, and three values of entry mass,  $m_e$ .

Table 3. Ballute Radius and Entry Mass Fraction for Neptune Aerocapture Ballutes, For Peak Ballute Temperature of 500 C.

Ve, km/s	emissivity	mass=100 kg		mass = 400 kg		mass = 1600 kg	
		radius m	mass fract ion, %	radius m	mass fract ion, %	radius m	mass fract ion, %
28.3	0.7	16-19	13-15	25-31	11-15	42-52	12-15.5
	0.5	20-24	16-19.5	32-38	16-21	50-62	15-19.5
32.0	0.7	21-25	17-20	35-40	18-22	61-69	19.5-23
	0.5	25-30	19.5-24	41-49	23.5-32	72-81	24.5-29.5

### FLOW FIELD STABILITY

Reference 8 has indicated that a disk or lens form ballute (Fig.1) will show interaction between the bow shock from the front payload body and the bow shock of the rear ballute body, in conditions where the payload shock is substantial. The remedy suggested is to have a ring or doughnut ballute shape. It is appropriate then to consider the Knudsen number of the payload during aerocapture and entry. The mean free path of the free stream near release of a typical ballute (number 4) is about 1 m, so that the flow then is approximately continuum, while it will be free-molecular on the tubing and intermediate on the orbiter. It is normally accepted that a Kn of 0.01 is necessary for a developed bow shock, and in the aerocapture case the ballute is probably released before this value is reached. In the entry case however, much of the drag occurs in developed continuum

conditions, and a ring shaped ballute is indicated. One way to determine how large a hole the doughnut should have is to fly ring ballutes with different hole sizes on a sounding rocket, to be deployed when in vacuum before reentering the atmosphere, and record the behavior on accelerators and with a camera. Conceptually the length of the tubing and net strands to the inner rings will be chosen so that the drag force tends to keep the ballute in the correct shape, even if the tubing disintegrates. A final test with actual high-speed real gas conditions should also be done to demonstrate that one has a stable ballute functioning as predicted here.

A thermal analysis of the system should be done. For aerocapture one is likely to find free-molecular conditions on the thin tubes used for deployment, which may also carry the strands of the g-load net, and to find continuum conditions on the ballute, while the payload body is in an intermediate regime. For an entry ballute similar conditions will be met briefly, and then all three objects - ballute, payload and tubing - will move towards continuum flow conditions. The consequences for heating are important. For example, the small objects (tubing and net strands) will have a heating limit at the low density for aerocapture, but not at later entry conditions during entry.

## BALLUTE MATERIAL DATA

The available data on strength versus temperature (Ref. 4) for Kapton and PBO seems to leave some questions unanswered. Kapton is available in films commercially down to thicknesses at or below the 7 micron (10 gm/m<sup>2</sup>) proposed here, and PBO is available commercially as fibers, and can be made in film form in limited quantities, with varying thickness in the range 10-30 gm/m<sup>2</sup>. Ref. 4 gives graphs for the tensile strength of PBO film and Kapton film (in the machine direction), and some values are shown in Table 5. In this paper the net, made of PBO, was evaluated with a cold strength of 56 kg/mm<sup>2</sup>, and the ballute fabric was assumed to be Kapton, 7 micron film with strength 5.6 ksi (3.943 kg/mm<sup>2</sup>) at 500 C. Ref. 4 gives a table comparing material properties, listing PBO with tensile strength of 56-63 kg/mm<sup>2</sup>, and gives a curve in the machine direction with the values of Table 4, as well as a strength of 820 ksi (576 kg/mm<sup>2</sup>) for high performance PBO fiber.

Table 4. Ballute Film Strength Versus Temperature.

Temperature deg C	Kapton film	Tensile strength, ksi and (kg/mm <sup>2</sup> )		
		PBO film (machine direction)	General PBO film	High performance PBO fiber
20	30.0 (21.1)	140 (98.4)	(56-63)	820 (576)
100	22.5 (15.8)	120 (84.4)		
200	15.3 (10.8)	90 (63.3)		
300	11.0 (7.7)	70 (49.2)		
400	7.9 (5.55)	65 (45.7)		
500	5.6 (3.94)	44 (30.9)		

It would seem that one could find high-performance PBO fibers for the ballute net that would be much stronger than the 56 kg/mm<sup>2</sup> assumed in this paper.

## DISCUSSION AND CONCLUSIONS

It can be seen that hollow disk-shaped ballutes for direct aerocapture at Neptune, for entry velocities in the range 28.3 to 32.0 km/s can be designed with Kapton fabric of mass 10 gm/m<sup>2</sup> and a maximum temperature of 500 C, and will have an entry mass fraction of about 14 % with an emissivity of 0.7 for entry mass of 100 kg to 1600 kg. The mass fraction rises to about 18% for emissivity 0.5. For entry speed 32.0 km/s and emissivity 0.7 the entry mass fraction is 18 % at entry mass 100 kg and 21 % for 1600 kg, and for emissivity 0.5 the mass fraction range is 22 to 27 %. Corresponding ballute radii range from 16 m for emissivity 0.7, mass 100 kg and entry velocity of 28.3 km/s to 81 m for entry mass 1600 kg, emissivity 0.5 and entry speed 32.0 km/s. For preliminary design with a margin one should take 20% mass fraction for low mass low speed entry and 30% for high mass high speed direct aerocapture at Neptune.

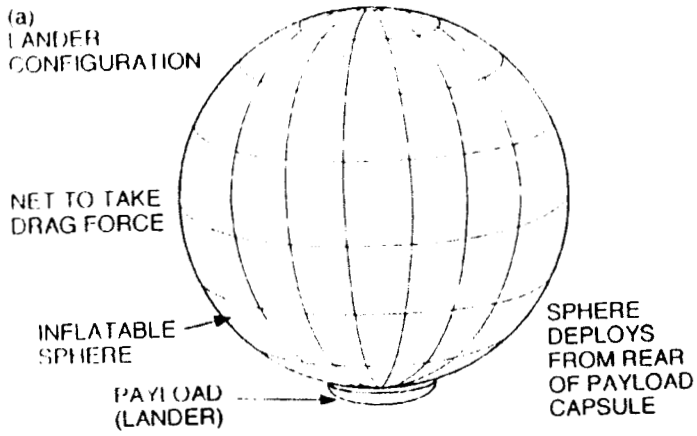
Evaluation of density and peak free-molecular and continuum heating rates to the ballute indicates that the mean free path is about 1 m for peak ballute heating and some tens of cm for peak g-load  $g_{max}$  and peak free-molecular heating  $q_{fm}$ . With a typical  $q_{ref}$  of 38.1 and  $q_{fm} = 11$  it can be seen that the tubing and the orbiter have peak heating rates of only a few W/cm<sup>2</sup>. The period of heating is typically 150 to 200 sec at ballute release, and 900 sec for a complete atmospheric pass. Because of its large size the maximum heating rate on the ballute is on the order of 1 or 2 W/cm<sup>2</sup>.

For ballutes to be ready for project use a development program must be followed to experimentally validate concepts for packaging and storing a large ballute for months, deploying it reliably in a matter of minutes prior to planetary entry, proving that the aerodynamic behavior is stable and predictable, and releasing it under the control of a reliable accelerometer integrator system. A ballute flight test as a Delta launch secondary payload in Earth reentry, or on a sounding rocket are being investigated.

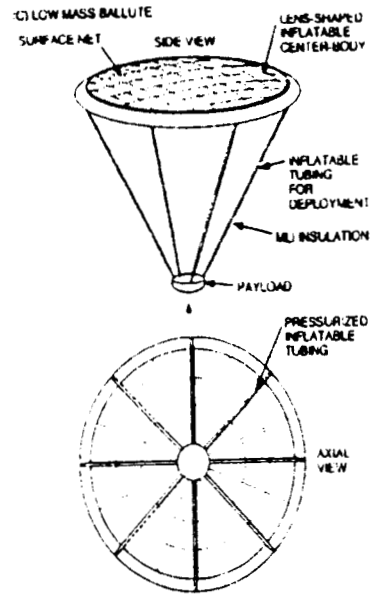
## REFERENCES

1. I.M.Jahemenko,"Ballute Characteristics in the 0.1 to 10 Mach Number Speed Range", J. Spacecraft, Vol. 4, No. 8, 1058-63, August, 1967.
2. L. D. Guy, "Structural and Decelerator Design Options for Mars Entry", J. Spacecraft, Vol. 6, No. 1, 44-49, January, 1969.
3. H. Akiba et al., "Feasibility Study of Buoyant Venus Station Placed by Inflated Balloon Entry", Paper at the 27th Int.Conf. Astronomy, Anaheim, Calif., October, 1976.
4. M.Murbach, NASA Ames, Private Communication, May 1999.
5. A.McRonald, "A Light-Weight Inflatable Hypersonic Drag Device for Planetary Entry", Paper at the Association Aeronautique de France Conf. at Arcachon, France, March 16-18, 1999.

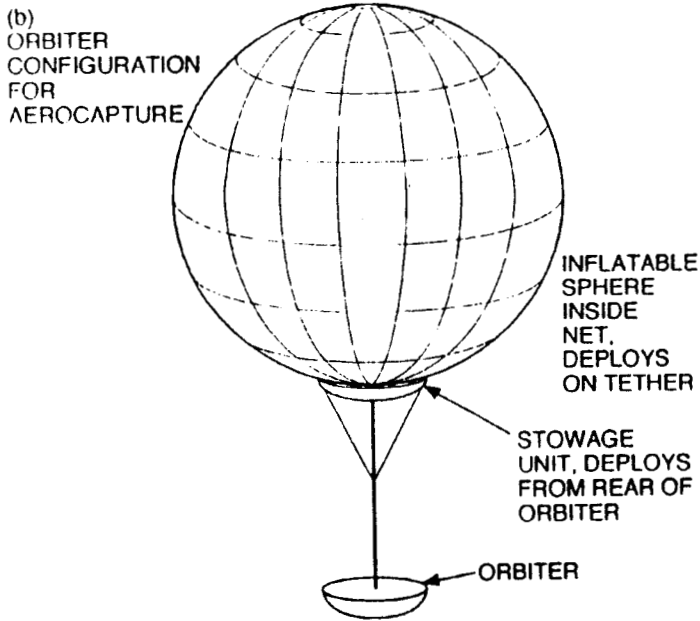
6. A. McRonald, "A Light-Weight Inflatable Hypersonic Drag Device for Venus Entry" Paper AAS 99-355 at the AAS/AIAA Astrodynamics Specialist Conf., Girdwood, Alaska, Aug 16-19, 1999., Paper at the AAS-AIAA Conf. in Alaska, August 1999.
7. A. Yavrouian et al., "High Temperature Materials for Venus Balloon Envelopes", AIAA Paper, 1995.
8. H. Hornung, California Institute of Technology, Private Communication, June 1999.
9. P.Gnoffo, NASA Langley, Private Communication, June 1999.
10. Glenn Orton, JPL, Private Communication, August 1994.
11. K. Sutton and R. Graves,"A General Stagnation-Point Convective-Heating Equation for Arbitrary Gas Mixtures", NASA TR-376, November, 1971.



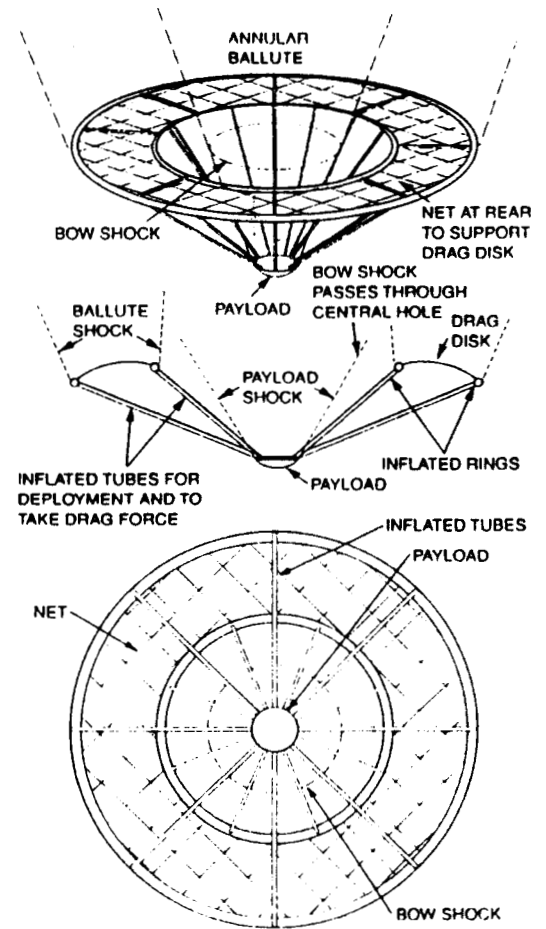
(a) Lander configuration



(c) Lens or Disk ballute



(b) Orbiter configuration



(d) Annular or Ring ballute

Fig. 1 Ballute configurations:

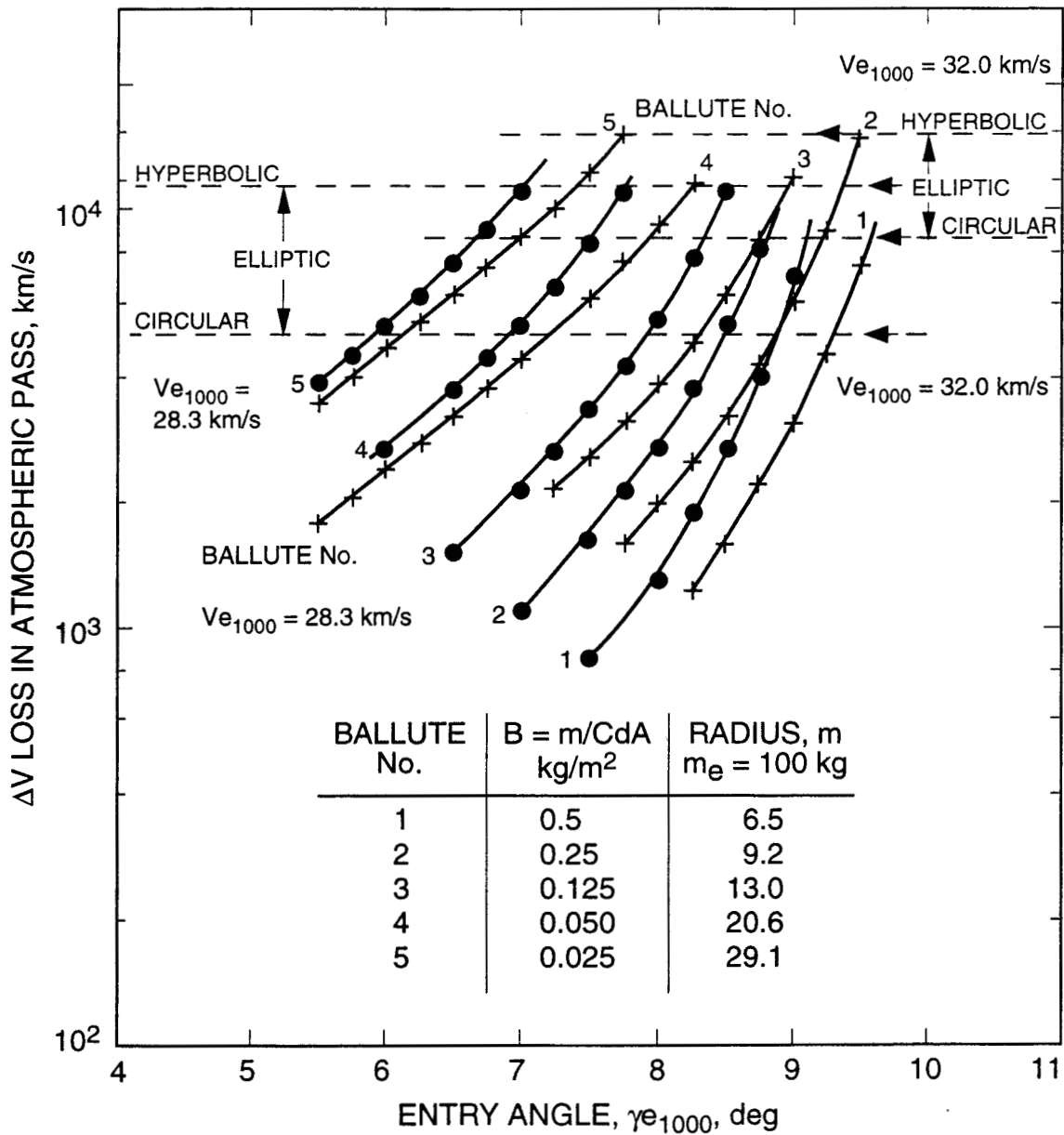


Fig. 2. Delta-V loss in an atmospheric pass versus entry angle, for ballutes in Neptune direct entry.

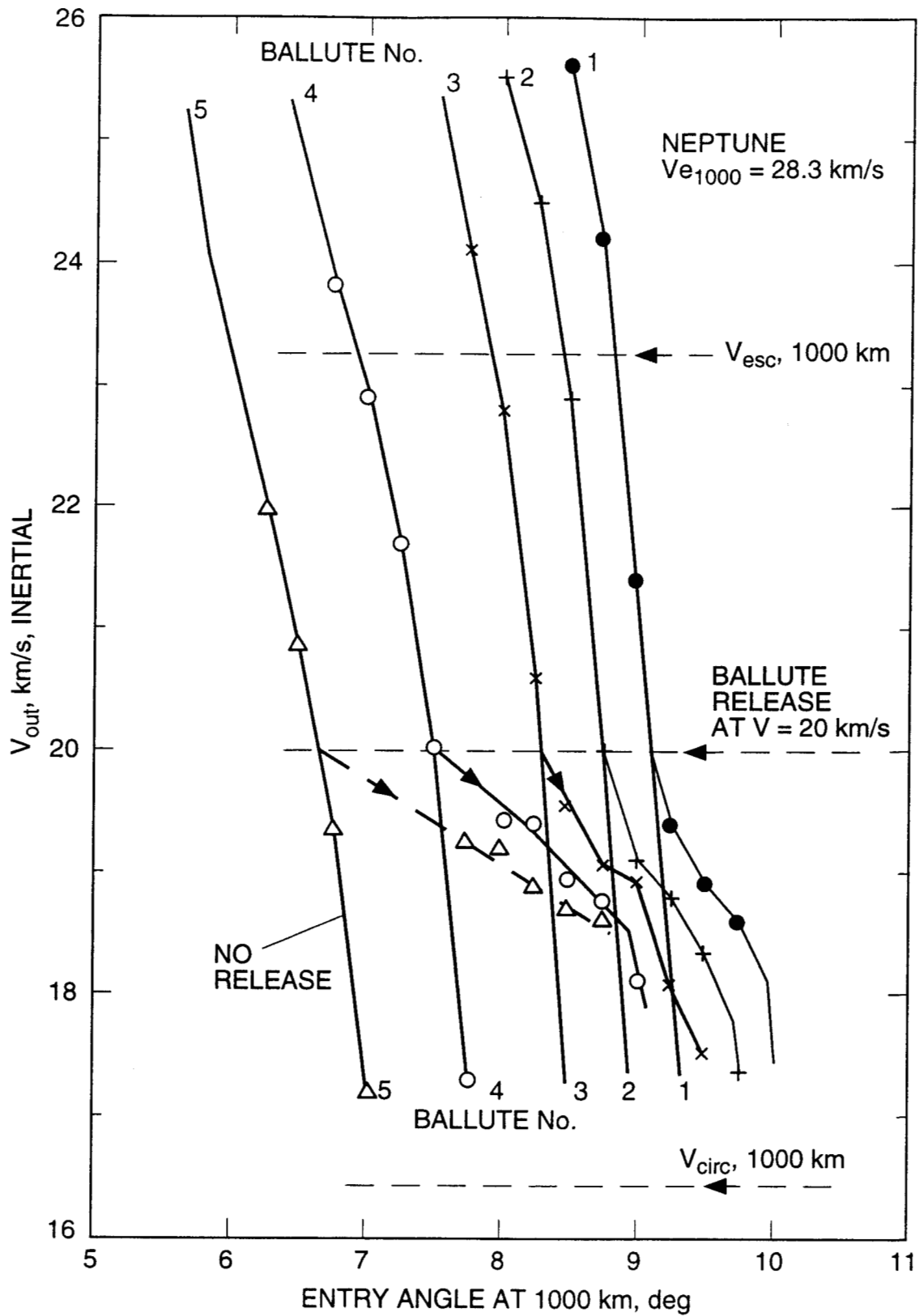


Fig. 3. Ballute exit velocity versus entry angle, with and without release, Neptune direct entry:  
 (a)  $V_e = 28.3 \text{ km/s}$ .

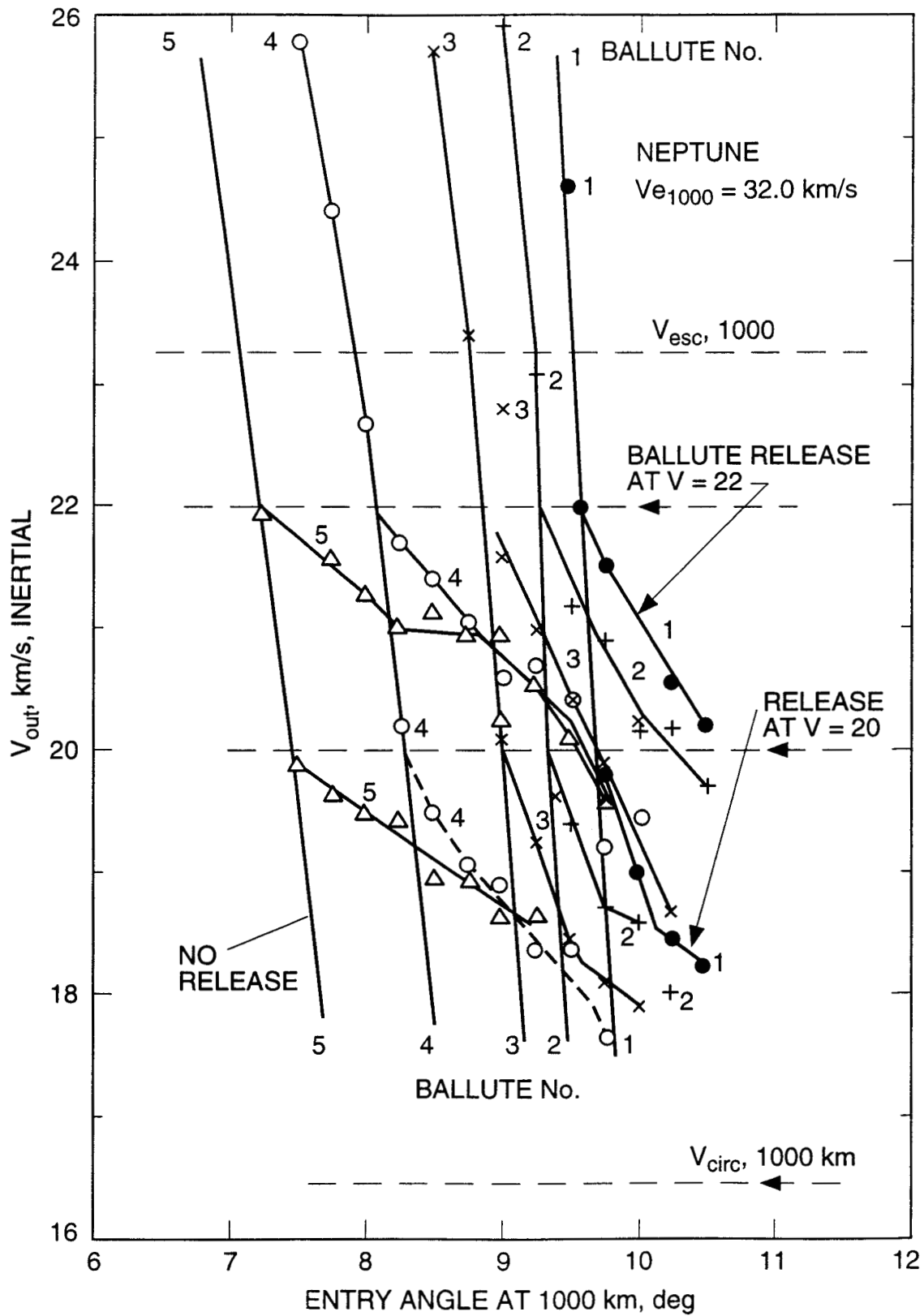


Fig. 3. Ballute exit velocity versus entry angle, with and without release, Neptune direct entry: (b)  $V_e = 32.0$  km/s.

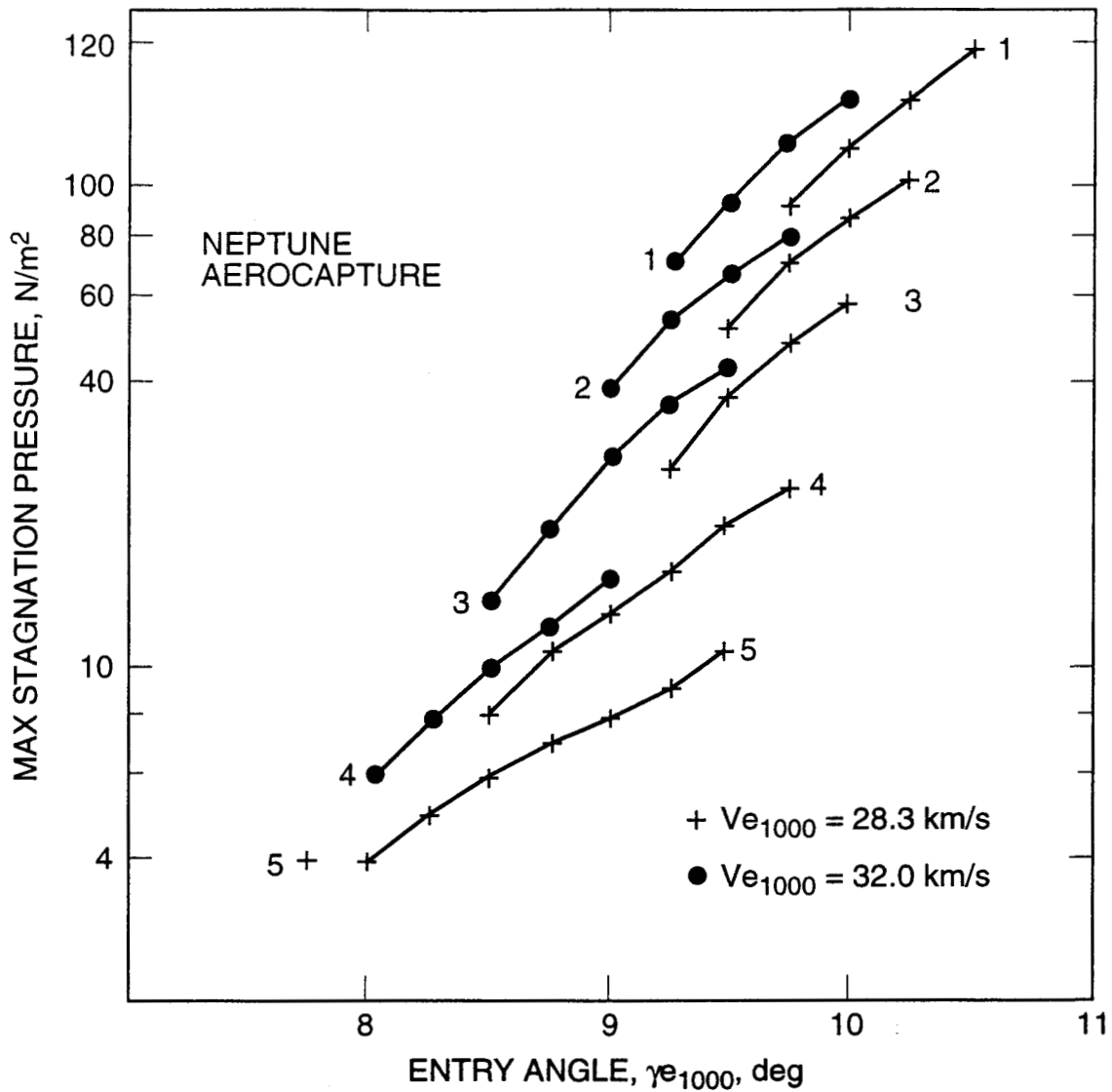


Fig. 4. (a) Peak stagnation pressure versus entry angle, Neptune direct entry.

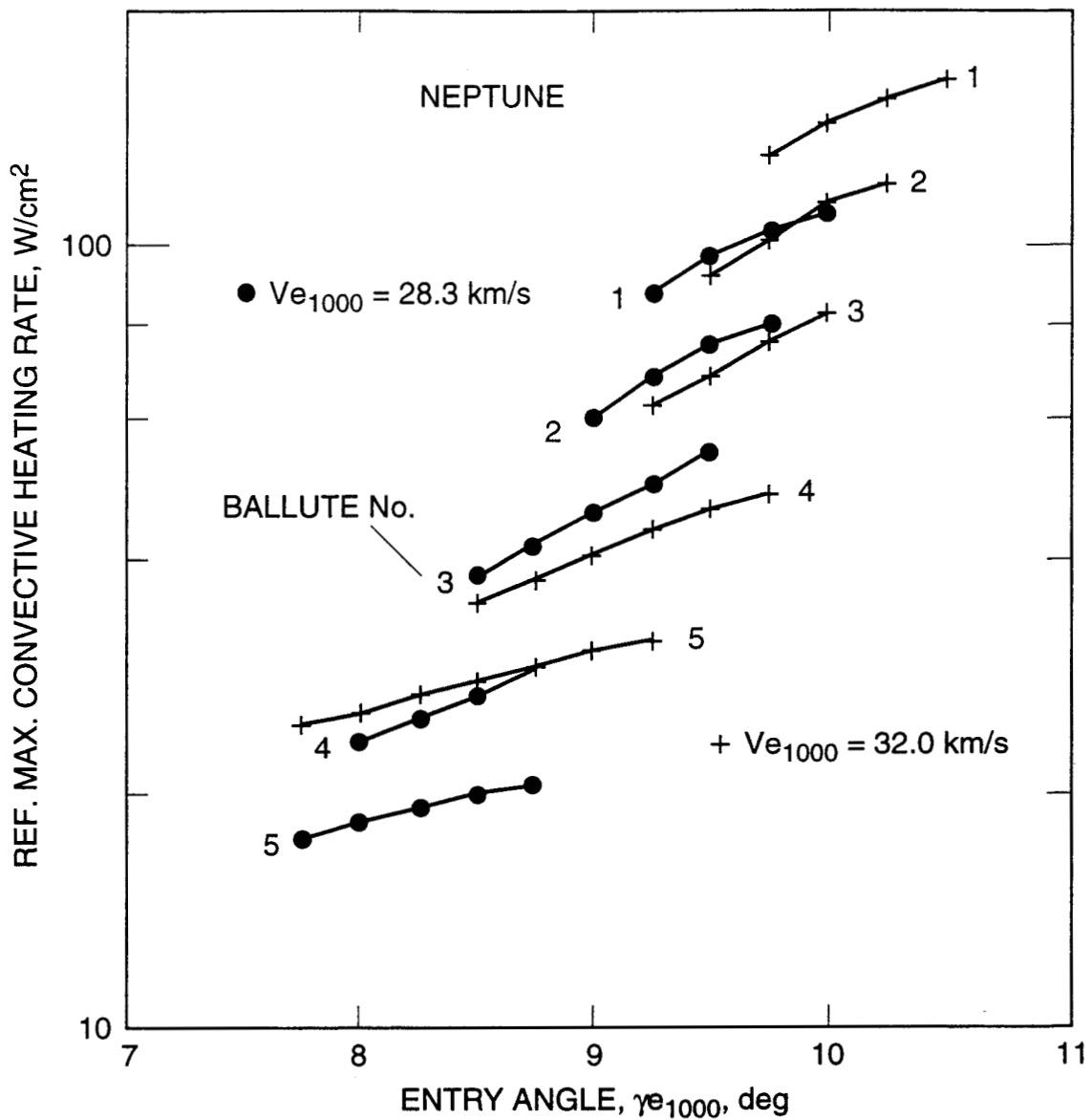


Fig. 4(b). Peak reference convective stagnation point heating versus entry angle, Neptune direct entry.

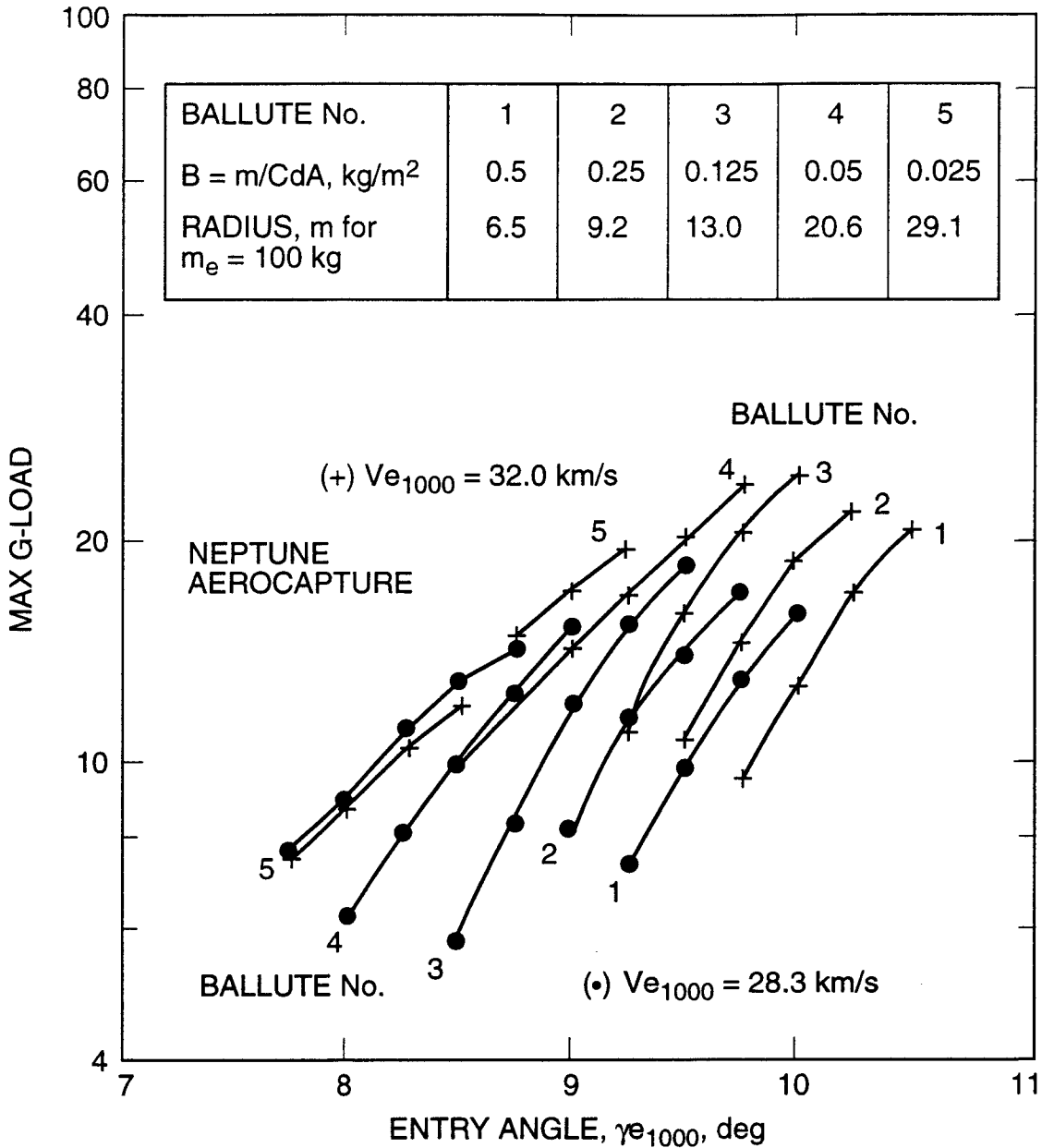


Fig. 4 ©. Peak g-load versus entry angle, Neptune direct entry.

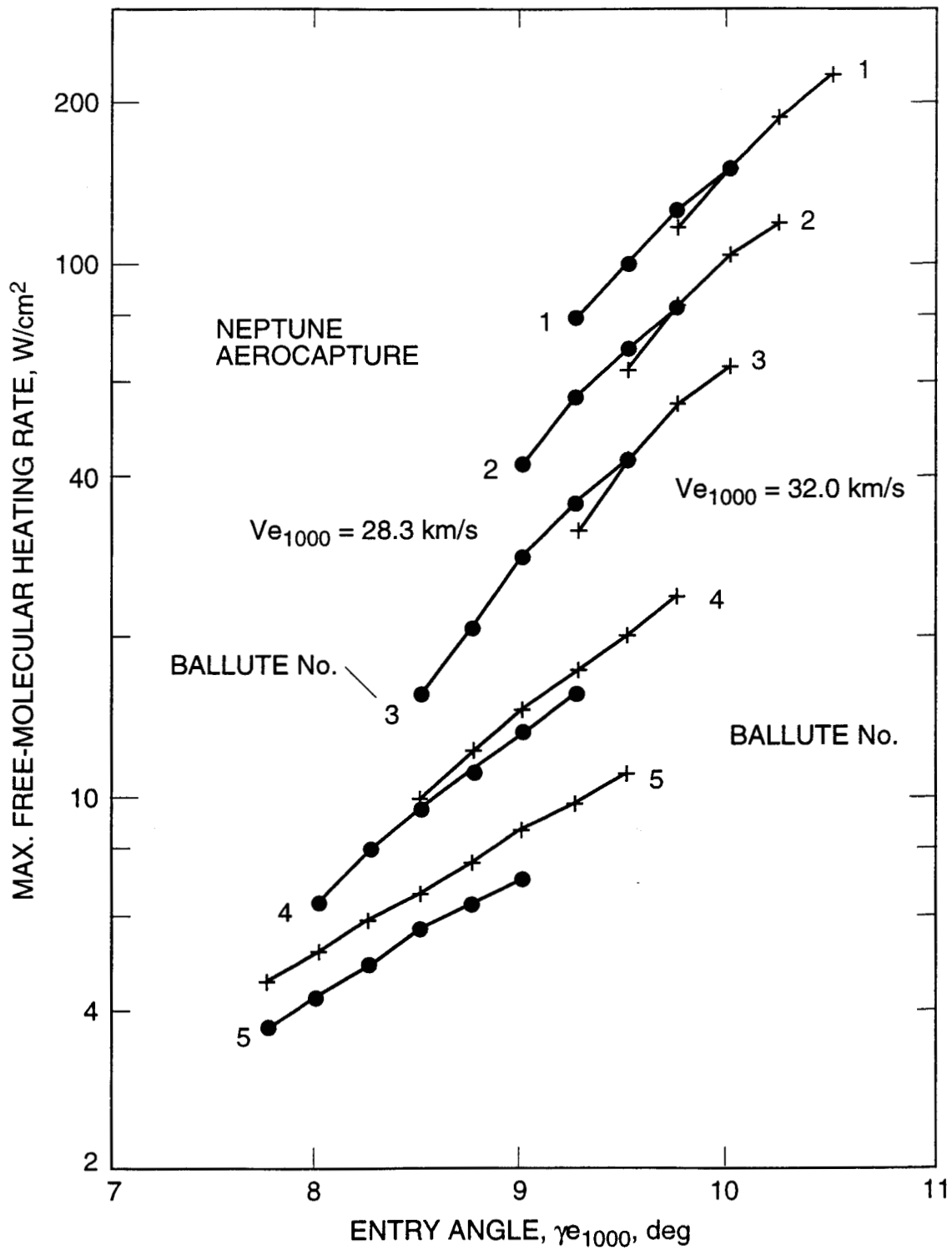


Fig. 4 (d) Peak free-molecular heating rate, Neptune direct entry.

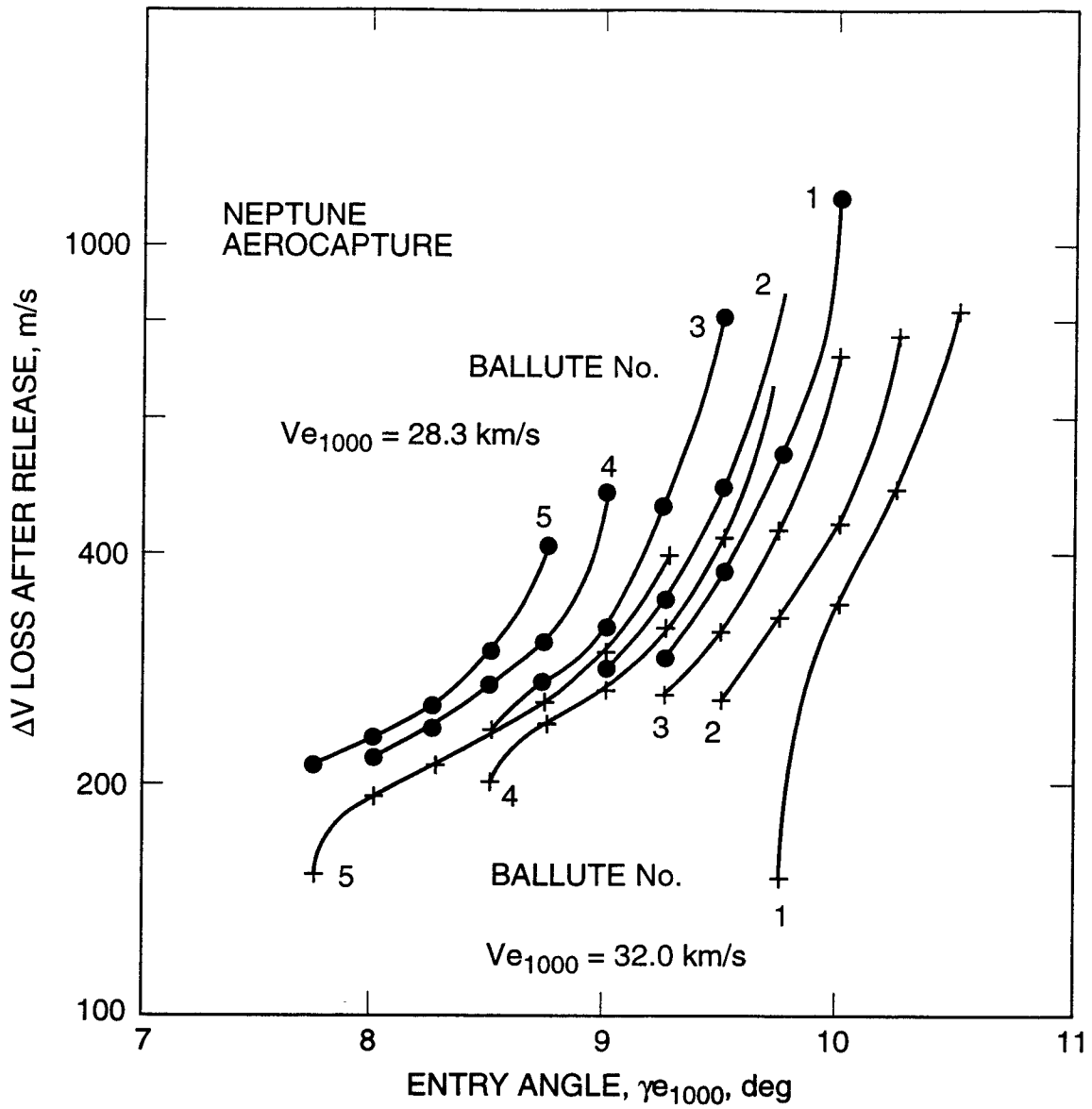


Fig. 5. Delta-V loss by orbiter after ballute release versus entry angle.

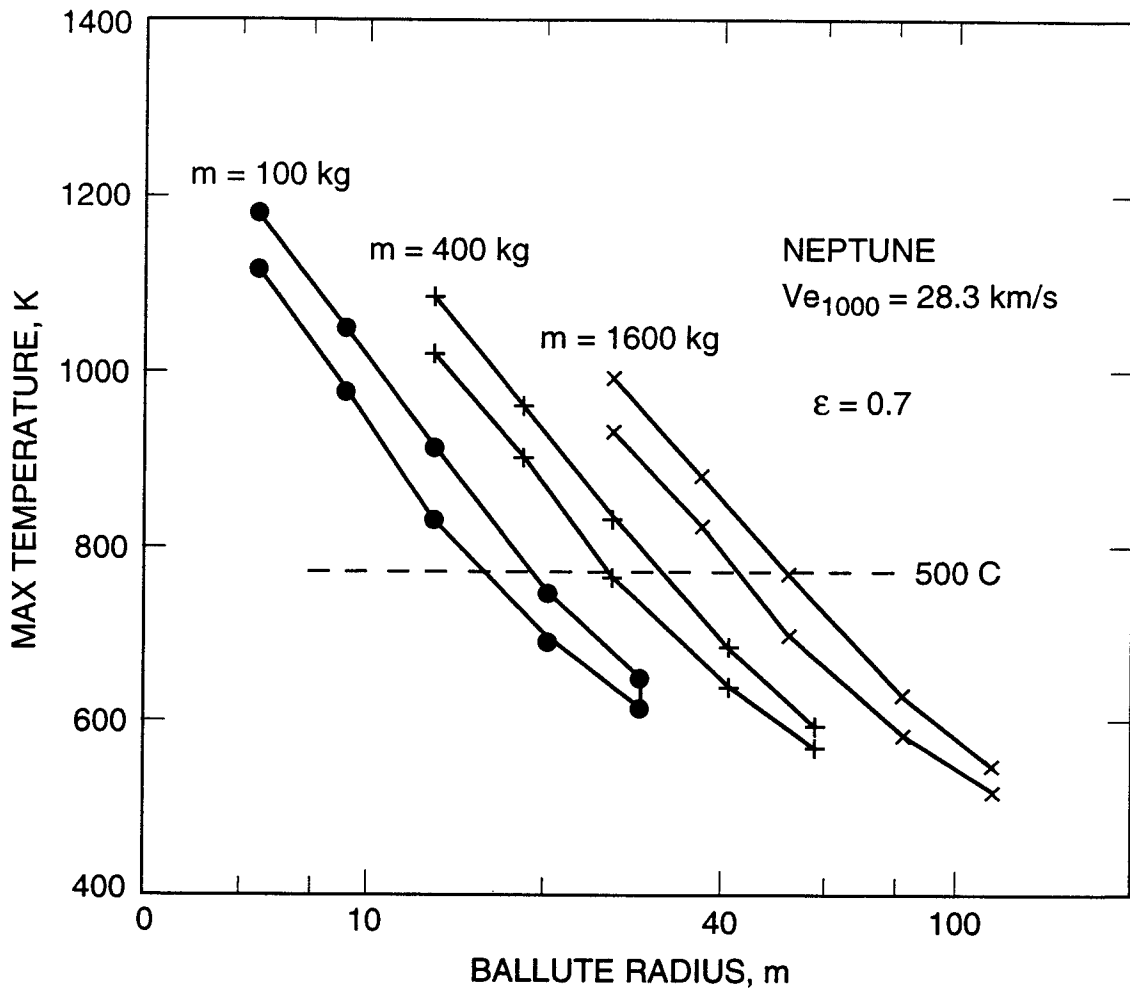


Fig. 6. Peak ballute temperature versus radius for several entry masses, Neptune direct entry :  
 (a)  $V_e = 28.3 \text{ km/s}$ , emissivity = 0.7.

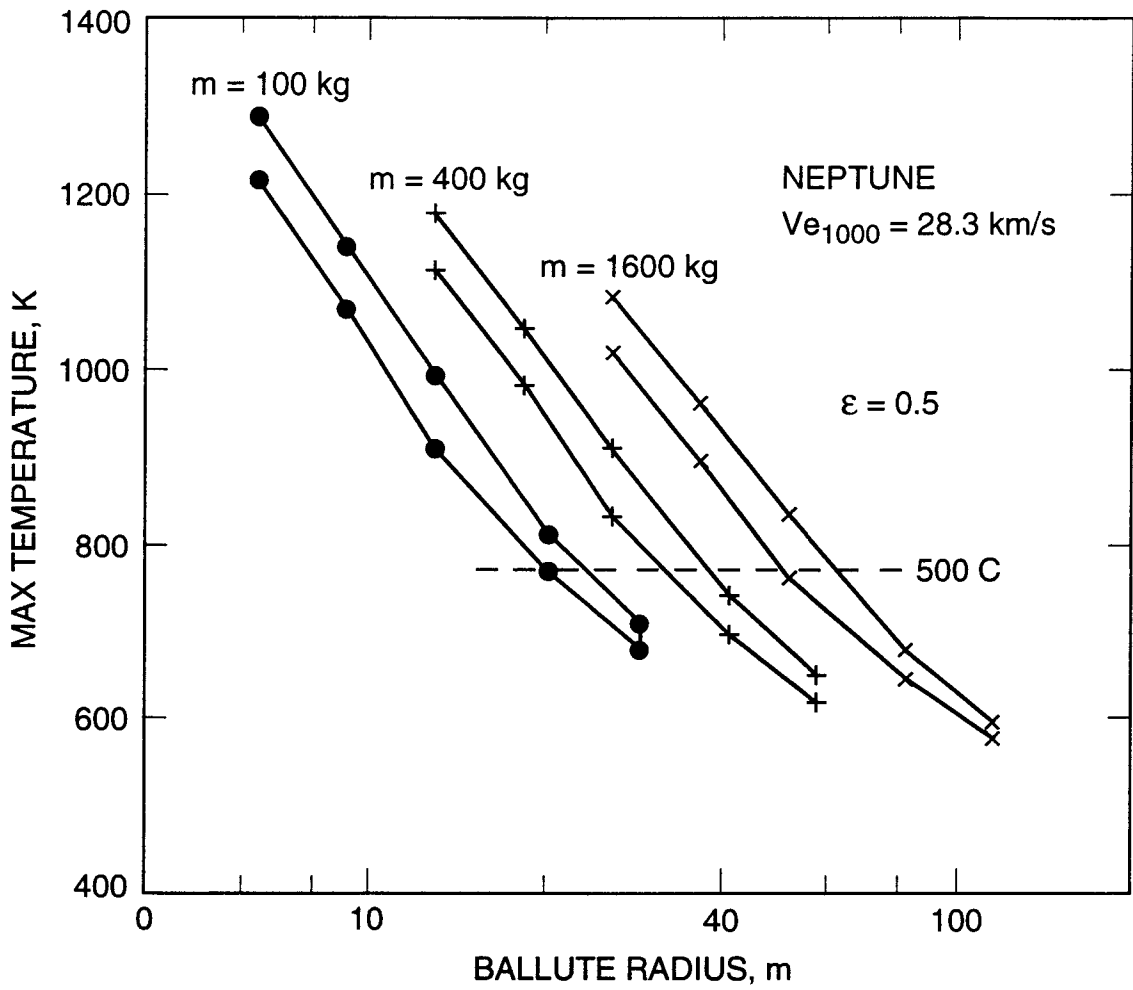


Fig. 6. Peak ballute temperature versus radius for several entry masses, Neptune direct entry :  
 (b)  $V_e = 28.3 \text{ km/s}$ , emissivity = 0.5.

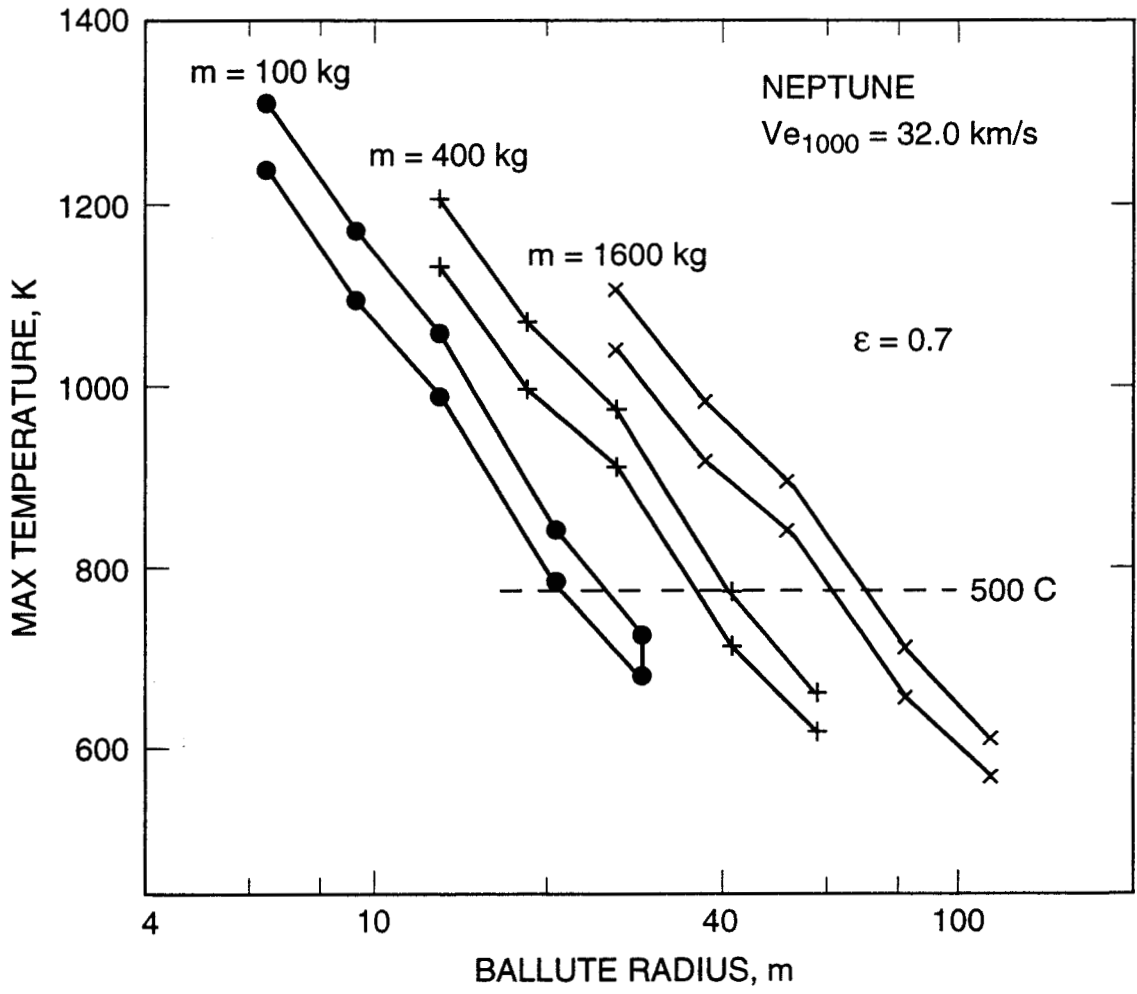


Fig. 6. Peak ballute temperature versus radius for several entry masses, Neptune direct entry :  
 © Ve = 32.0 km/s, emissivity = 0.7.

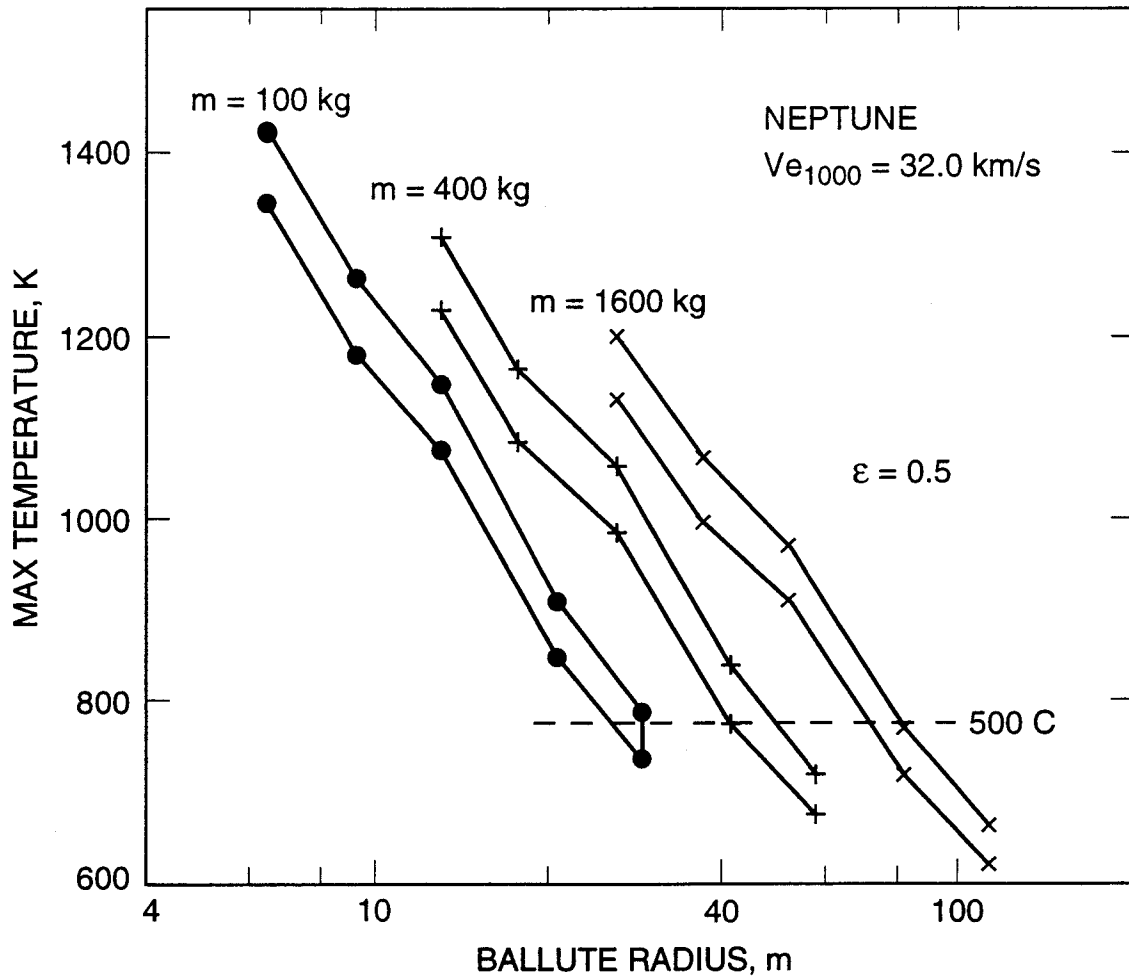


Fig. 6. Peak ballute temperature versus radius for several entry masses, Neptune direct entry :  
 (d)  $V_e = 32.0$  km/s, emissivity = 0.5.

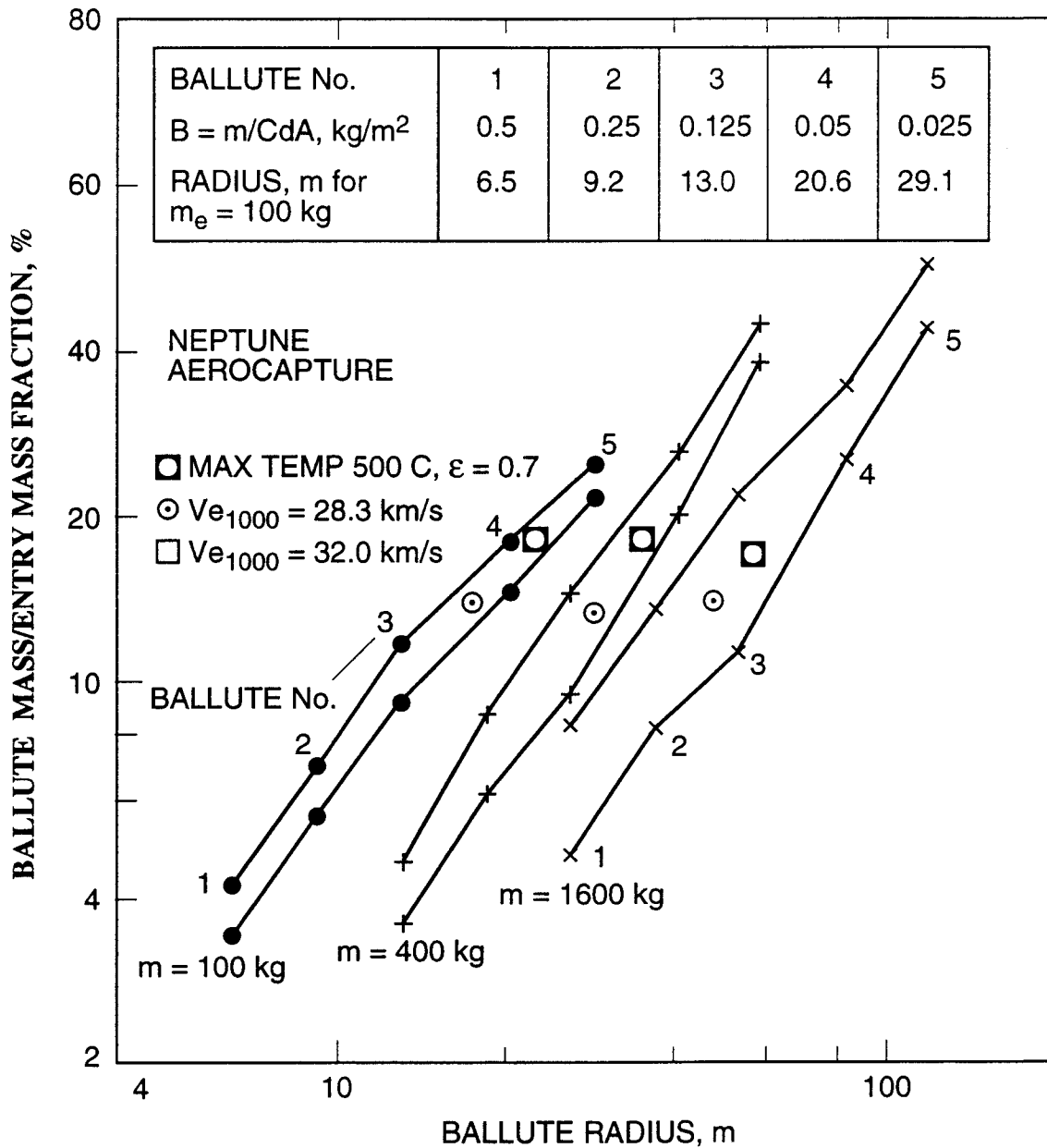


Fig. 7. Ballute mass fraction (ballute mass/entry mass) versus radius for several masses, Neptune direct entry.